Comparison of organic Rankine cycle concepts for recovering waste heat in a hybrid powertrain on a fast passenger ferry

Norbert Lümmen*, Erlend Nygård, Peter E. Koch, Lars M. Nerheim

Department of Mechanical and Marine Engineering, Western Norway University of Applied Sciences, Postboks 7030, 5020 Bergen, Norway

Abstract

The possibilities of recovering waste heat from the exhaust gas and other waste heat sources from a 900 kW fast passenger ferry Diesel engine by means of an organic Rankine cycle (ORC) were investigated. The recovered energy is to be used in a parallel hybrid powertrain, which would allow for electric propulsion and thus low emissions near stopovers while electricity generated by the ORC when the engine is running at cruising speed is stored in a battery. The benefit of such a solution is that there would be no extra load on the engine and increased fuel consumption while the local emissions around the stopovers could be reduced, which is especially desirable in urban environments. Simple organic Rankine-cycles with and without internal energy regeneration and an organic Rankine cycle with two different heat sources have been modelled. Different working fluid candidates have been compared by means of a simple optimization routine with respect to the maximum recoverable amount of work from the cycles' expander. The method is applied to a vessel serving a typical short fast passenger ferry route between the harbour of the Western Norwegian city of Bergen and the neighbouring Askøy municipality.

Highlights

- Models for simple, regenerative and double-source organic Rankine cycle (ORC)
- Comparison of different working fluids
- Optimization for maximum net power output
- Unconstrained and constrained expansion compared
- ORC-based energy recovery for electric propulsion possible in certain scenarios

Keywords: marine Diesel engine, waste heat recovery, organic Rankine cycle, optimization, fast passenger ferry

*Corresponding author: Norbert Lümmen, nlu@hvl.no

Introduction

Fast passenger ferries are an important means of transport along the Norwegian coast and many other places in the world. Increased environmental awareness has shed light on the gaseous and particular emissions from the internal combustion engine in general, and especially when such vessels navigate close to land before and after mooring at a stopover. There are about 30 fast passenger ferry routes in Norway. Most of these routes are served by catamarans with speeds above of 20 kn. Even though only 1.8 % [1] of all passengers traveling by means of public transport (ca. 625 million [1]) in 2016 were travelling on a sea route, it is in many regions the only convenient means of transport.

Electric propulsion with energy stored in a battery from either charging from a land connection during a stopover, charging the battery with the main engines running a generator, and generating electricity by recovering thermal energy from on board waste heat sources are possible scenarios. The authors have investigated the latter of these three cases. The result is a parallel hybrid powertrain, which adds an electric motor to drive the propeller shaft, which is powered by a battery. In case the energy recovered during cruising between stopovers is not enough for manoeuvring and transit of the harbour at a stopover, a plugin option can be added to allow for additional battery charging from a landline.

The majority of published investigations cover waste heat recovery (WHR) from exhaust gases of internal combustions engines by either organic Rankine cycle (ORC) [2], thermoelectric generator (TEG) [3] or turbo-generator (TG) [4]. The recovered energy is usually converted into electricity for direct use or storage in a battery. On larger ocean going ships, waste heat recovery is a measure to increase a vessel's Energy Efficiency Design Index (EEDI). The International Maritime Organization (IMO) established this index as a means to compare ships of different design and construction dates and use this as a basis for requirements for improvements in energy efficiency over the coming years.

Pili et al. investigated the suitability of ORC-WHR-solutions for different mobile applications like city busses, heavy cargo trucks (40 t), freight trains (1000 t), inland water (2500 t) and ocean vessels (25000 t) [5]. ORCs were found to be highly applicable for maritime transportation. Freight trains and

cargo trucks were on the boundary of what is economically feasible when ORCs are retrofitted to existing vehicles and vessels. While many studies focus on the exhaust gas as sole source of waste heat [6, 7] it could be shown the engine cooling water with temperatures between 80 °C and 95 °C can also be a useful waste heat source [8]. About 120 kW could be recovered from about 1.94 MW of thermal energy available in the engine cooling water on the cargo ship *Arnold Maersk*, which has a 72 MW 12-cylinder engine. Both Yang & Yeh [9] and Song et al. [10] have studied ORC models in which both engine cooling water and exhaust gas were used as waste heat sources. Both studies contain models in which the engine cooling water is employed for both preheating and evaporating the ORC-working fluid. The study by Song et al. [10] also has a model where two separate ORCs with different working fluids are used with one recovering energy from the engine cooling water and the other one recovering energy from the exhaust gases.

Zhao et al. conducted performance simulations of a six-cylinder four-stroke turbocharged Diesel engine for a heavy truck with 258 kW rated power that was extended with an ORC [11]. The simulation model was implemented in Simulink and the results were validated experimentally. Transient performance simulation results showed that the effects of an ORC system on the acceleration performance of an engine are minimal. Scaccabarozzi et al. [12] compared pure working fluids to zeotropic mixtures in ORCs recovering energy from two 10 MW two-stroke engines with different exhaust gas temperatures. Several parameters of an ORC like condenser pressure, turbine inlet pressure and superheat temperature were optimized by means of evolutionary algorithms. It was found that the use of optimized mixtures lead to an increase in power output and thus exergy efficiency.

The aim of this study is to find out if enough energy can be recovered from waste heat on board a fast passenger ferry by means of an organic Rankine cycle. The vessel operates on a short fjord-crossing route. The recovered energy is to be stored in batteries in order to be able to navigate under electric propulsion near the two stopovers. The vessel serving as the case study (MS Teisten) is a catamaran

built in 2006, which is equipped with 4 MTU 10V 2000M72CR Diesel engines [13]. The nominal power of each engine is 900 kW at 2250 rpm. Engines of similar power in other studies operate at lower rpm (1500 rpm, for example [5, 10, 14]), and are mounted on other types of vessels. There are two engines in each hull, which are both coupled to the same shaft. In each hull, one engine is actively running, the other is for redundancy. The vessel has a length of 30 m, a beam of 4.5 m, displacement of 106 m^3 and a capacity of 180 passengers. The cruising speed during a fjord crossing is 26 kn while the maximum speed is 35 kn.

The article is structured as follows: At first data on the vessel, its engines and the route it operates on is given. After that, the necessary equations for the three different types of ORC models are derived. This part is followed by a selection of working fluids to be considered in the analysis. The results of the optimization of the different types of cycles are presented and discussed before conclusions are drawn.

Data

The case studied in this investigation is a short connection across the fjord between the city of Bergen on the east side and the Askøy municipality on the West side. A minimum of 21 fjord crossings are carried out per weekday. The shortest time interval between two departures from the same port is 30 min.

Figure 1 shows a power profile for one fjord crossing from Bergen to Askøy [15].

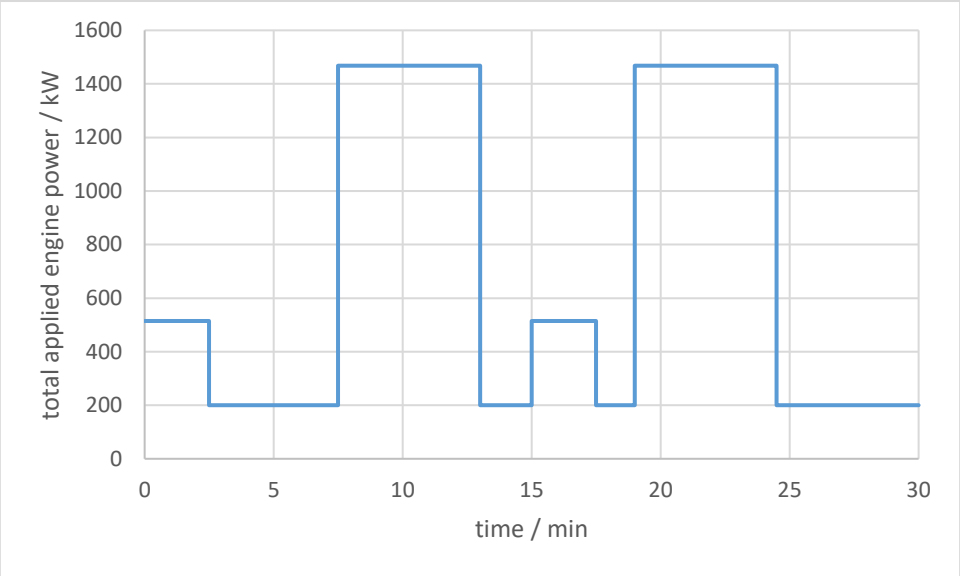

Figure 1: Power profile for a single fjord crossing from Bergen to Askøy and back. Shown are the mechanical energy need during the different phases of the passage. The high-energy need at the beginning and from 15 min to 17.5 min is due to thrusting against the quay at a stopover instead of mooring with lines.

The total necessary engine power during harbour transit is $\dot{W}_{\mathrm{harbour}} = 200$ kW [15], while $\dot{W}_{\mathrm{cruising}} = 1468$ kW are used during acceleration and fjord crossing at constant speed (which is 81.6% of the theoretical engine power from the two 900 kW engines).

The necessary time for manoeuvring and transit in harbour in Bergen are 1.5 min and 3.5 min (due to a speed limit of 5 kn within the harbour boundaries), while there is only 1.5 min of manoeuvring in the other harbour (Askøy). This gives a total time of $\Delta t_{\mathrm{harbour}} = 13$ min at 200 kW for both harbours on a round-trip. The transit time in each direction is 0.5 min of acceleration and 5 min at fjord crossing speed. The total time at maximum utilized engine power is therefore $\Delta t_{\mathrm{cruising}} = 11$ min. Time at the quay is equal at both stopovers and of 2.5 min duration.

Model

The model used in the calculations of extractable energy from the exhaust gas flow is based on the subcritical ORC-model by Mikielewicz & Mickielewicz [16]. In contrast to the original model, some enthalpy differences were kept and not replaced by products of heat capacities and temperature

differences. Three different types of setups are analysed. A simple ORC, a regenerative ORC, and a simple ORC with two different heat sources (double source ORC). All three models are for subcritical cycles, which means that the maximum pressure is lower than the working fluid's critical pressure. The different types are discussed in the next subsections. For each both a sketch of the different components and a *T*-*s*-diagram showing all involved mass-flows is given. The full set of equations is given for the simple ORC. For the other two ORC-types, only the equations which differ from the simple ORC are listed. The models for the simple and the regenerative ORC are similar to those employed by Michos et al. [14], who used a heat transfer fluid (thermal oil) between waste exhaust gas and ORC-working fluid in addition. The double source ORC is similar to the model employed by Yang and Yeh [9] and the optimized model used by Song et al. [10], which have both used the engine cooling water not only for preheating but also for evaporating the ORC-working fluid. This aspect is different in the presented work, where the engine cooling water is only used for preheating the ORC-working fluid.

Table 1 gives an overview over the necessary input data to the equations of the model, which has been realized in Microsoft Excel® with the CoolProp add-on [17].

Table 1: Input data to the work sheet where the optimisation is carried out.

Fluid	Property	Comment
ORC-working fluid	$P_{\max}, P_{\min}$	Maximum and minimum pressure in the cycle; later varied by the solver within given constraints. $P_{\max}$ is the pressure between pump outlet and expander inlet, $P_{\min}$ is the pressure between expander outlet and pump inlet.
	$T_{\max,\mathrm{ORC}} = T_1$	Temperature at expander inlet (max. temperature of ORC-fluid); later varied by the solver within given constraints; maximum value set to 300 °C.

	ε	Efficiency of the recuperator in the regenerative ORC; set to 0.8.
	$\eta_{s,\text{pump}}, \eta_{s,\text{exp.}}$	Isentropic efficiencies of pump and expander; set to 0.85 and 0.9 respectively.
	$\Delta T_{\text{superheat,min.}}$	Minimum superheating over saturation temperature at $P_{\max}$; used to guarantee dry vapour at expander inlet and set to 0.05°C.
	$\Delta T_{\text{pp,source,min}}$	Minimum temperature difference between working fluid and heat source fluid during heating and evaporation; set to 5°C; used as constraint.
	$\Delta T_{\text{pp,sink,min}}$	Minimum temperature difference between working fluid and heat sink fluid during condensation; set to 5°C; used as constraint.
	$\Delta T_{\text{pp,low } T,\text{min}}$	Minimum temperature difference between working fluid and low temperature heat source fluid (double source ORC only); set to 5°C; used as constraint.
Waste heat fluid (high temperature)	$T_{\text{max, source}} = T_6$	Maximum temperature of the heat source fluid
	$T_{\text{min, source}} = T_{9a/9b}$	Minimum allowable temperature in heat source fluid; used as constraint.
	P_{source}	Pressure in all states of the heat source fluid
	M	Molar mass
	R	Individual gas constant
	$c_{P,\text{source}}$	Specific heat capacity at constant pressure

	$\dot{m}_{\text{source}}$	Mass flow
Waste heat fluid (low temperature; double source ORC only)	$T_{\text{max, low } T} = T_{14}$	Maximum temperature of the low temperature waste heat fluid (double source ORC only)
	$\Delta T_{\text{max, low } T}$	Maximum allowed temperature drop
	$c_{P,\text{low } T}$	Specific heat capacity of at constant pressure
	$\dot{m}_{\text{low } T}$	Mass flow
	$P_{\text{max, low } T}$	Pressure in both states of the low temperature fluid
Heat sink fluid	$T_{\text{min, sink}} = T_{11}$	Minimum temperature in heat sink fluid; initially set to T_0
	$P_{\text{sink}} = P_{11}$	Pressure used in all states of the heat sink fluid
	$\Delta T_{\text{condens.}} = T_{2'} - T_{11}$	Difference between inlet temperatures for working fluid and heat sink fluid in condenser; set to 15 °C
	$\Delta T_{\text{heat sink,max}}$	Maximum allowed temperature rise in heat sink fluid. It is set to 20 °C.
Surroundings	T_0, P_0	Temperature and pressure of the surroundings

In principle, different mass flows are available around a marine Diesel engine that may be used as heat source fluid. These are the exhaust gases, the lubricant (oil) and engine cooling liquid. When the exhaust gases are used as heat source fluid in the calculations they are assumed to behave like an ideal gas with constant specific heat capacities at the average temperature of $T_{\text{max, source}}$ and $T_{\text{min, source}}$. Molar mass, individual gas constant and specific heat capacity are calculated based on a volumetric analysis of the exhaust gas composition, where the main compounds N_2, CO_2, H_2O and O_2 are accounted for. In the case of oil and cooling fluid, the compressed liquid phase at a given pressure is

assumed for these fluids throughout the heat exchanging process. The same is done for the heat sink fluid, which is treated like seawater at an assumed annual average temperature of 10°C with a specific heat capacity of 4.003 kJ/(kg·°C). It is assumed that all these liquids can be treated as incompressible fluids. Values for the specific heat capacity at constant pressure are used for the respective average temperatures in the heat exchanging processes these fluids are involved in. In general, pressure losses in all fluids are neglected. The same maximum pressure is used in all states between the outlet of the pump and the inlet of the expander and the same minimum pressure is applied in all states between the expander outlet and the pump inlet.

Simple ORC

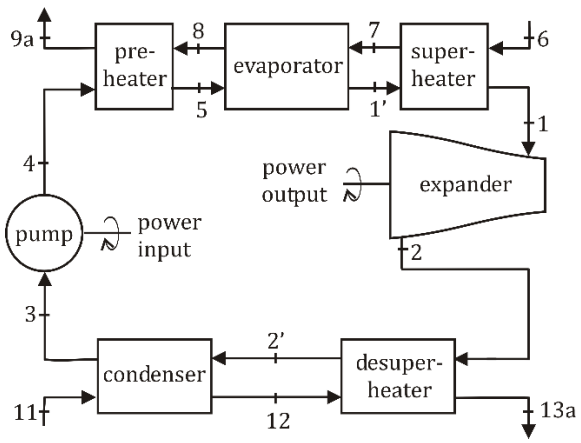

Figure 2: Setup of the simple ORC with a single waste heat fluid and heat sink

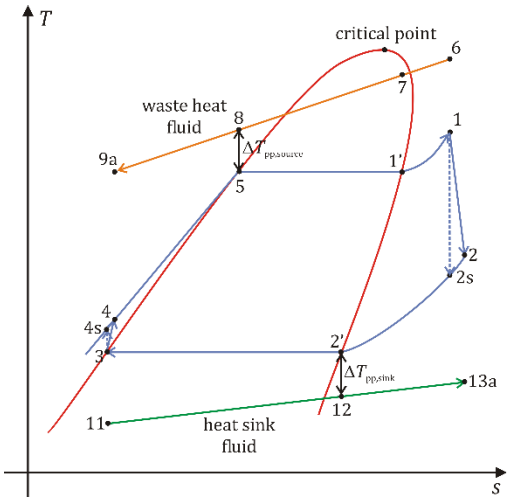

Figure 3: T-s- diagram for the simple ORC.

The following equations are used in the calculation of state properties in the different fluid. Based on the ORC-working fluid properties in state 1, the specific enthalpy in state 2 (expander outlet) is calculated by

$$h_2 = h_1 - \eta_{s,\text{exp.}}(h_1 - h_{2s}) \tag{1}$$

Where h_{2s} is the specific enthalpy in case of isentropic expansion between the pressures in states 1 and 2.

It is assumed that the ORC-working fluid is in the saturated liquid phase at the inlet of the pump at $P_{\min}$. The specific enthalpy at the pumps outlet is

$$h_4 = h_3 + \frac{(h_{4s} - h_3)}{\eta_{s,\text{pump}}} \tag{2}$$

where h_{4s} is the enthalpy at the pump outlet for isentropic compression.

The working fluid reaches its saturated liquid phase in state 5. The saturated vapour phase is designated state no. 1'.

The heat source fluid enters the heat exchanger, which is the evaporator for the working fluid, in state 6 with given temperature, pressure and mass flow $\dot{m}_{\text{source}}$. Its temperature drops to

$$T_7 = T_8 + \frac{\dot{m}_{\text{ORC}}(h_{1'} - h_5)}{\dot{m}_{\text{source}} c_{P,\text{source}}} \tag{3}$$

In state 8, which is the pinch point between working fluid and heat source fluid, the temperature has further dropped to

$$T_8 = T_5 + \Delta T_{\text{pp,source}} \tag{4}$$

where the current pinch point temperature is $\Delta T_{\text{pp,source}}$, which is varied by the solver. In case of a simple ORC, the heat source fluid temperature at the outlet of the preheater is

$$T_{9a} = T_6 - \frac{\dot{m}_{\text{ORC}}(h_1 - h_4)}{\dot{m}_{\text{source}} c_{P,\text{source}}} \geq T_{\text{min, source}} \tag{5}$$

A minimum temperature value constraint has to be defined for the heat source fluid ($T_{\text{min, source}}$) and T_{9a} must not be lower than that. The reason is that a certain temperature must be kept for the exhaust

gas cleaning system to work properly. This temperature lies typically between 300 – 330 °C. To have some safety margin, $T_{\text{min, source}}$ = 350 °C was used.

The heat sink fluid enters the low temperature side of the working-fluid-condenser at $P_{\text{sink}} = P_{11}$ and $T_{\text{min,sink}} = T_{11}$. At the pinch point with the working fluid, the temperature has increased to

$$T_{12} = T_{2'} - \Delta T_{\text{pp,sink,min}} \tag{6}$$

In a simple ORC, the heat sink fluid temperature at the outlet of the condenser is

$$T_{13a} = T_{12} - \frac{\dot{m}_{\text{ORC}}(h_{2'} - h_2)}{\dot{m}_{\text{sink}} c_{P,\text{sink}}} \tag{7}$$

In the both simple and regenerative ORC setup, the mass flow rate of the working fluid is calculated by

$$\dot{m}_{\text{ORC}} = \dot{m}_{\text{source}} c_{P,\text{source}} \frac{(T_6 - T_8)}{(h_1 - h_5)} \tag{8}$$

The corresponding mass flow rate of the heat sink fluid is

$$\dot{m}_{\text{sink}} = \dot{m}_{\text{ORC}} \frac{(h_2 - h_3)}{c_{P,\text{sink}} \Delta T_{\text{heat sink,max}}} \tag{9}$$

The maximum available heat transfer rate from heat source to working fluid is

$$\dot{Q}_{\text{source}} = \dot{m}_{\text{source}} c_{P,\text{source}} (T_{\text{max}} - T_{\text{min}}) \tag{10}$$

where $T_{\text{max}} = T_6$ for both the simple and regenerative ORC, and $T_{\text{min}} = T_{9\text{a}}$ for the simple and $T_{\text{min}} = T_{9\text{b}}$for the regenerative ORC, respectively. The recovered exergy rate is equal to the net work output from the ORC and given by

$$\dot{X}_{\text{recovered}} = \dot{W}_{\text{net,out}} = \dot{m}_{\text{ORC}}[(h_1 - h_2) - (h_4 - h_3)] \tag{11}$$

where the first specific enthalpy difference on the right hand side is the specific work output from the expander and the second specific enthalpy difference is the specific work input to the pump. The heat rejection rate from the working fluid in the condenser is

$$\dot{Q}_{\text{sink}} = \dot{m}_{\text{ORC}}(h_2 - h_3) \tag{12}$$

The total available exergy rate of heat source fluid is given by

$$\dot{X}_{\text{source,total}} = \dot{m}_{\text{source}} \left[c_{P,\text{source}}(T_6 - T_0) - T_0 \left(c_{P,\text{source}} \ln \frac{T_6}{T_0} - R \ln \frac{P_6}{P_0} \right) \right] \tag{13}$$

while the available exergy for recovery by the ORC is limited by the allowed temperature drop in the exhaust gases, which is set to $T_{\text{min}} = T_{9a}$. It is therefore given by the exergy rate change of the heat source fluid

$$\dot{X}_{\text{source,available}} = \dot{m}_{\text{source}} c_{P,\text{source}} \left[(T_6 - T_{9a}) - T_0 \ln \frac{T_6}{T_{9a}} \right] \tag{14}$$

Where the natural logarithm of the pressure ratio between the two involved states vanishes because of the assumption of zero pressure drop in the heat sink fluid.

The thermal efficiency of the ORC is defined as

$$\eta_{\text{th}} = \frac{\dot{W}_{\text{net,out}}}{\dot{Q}_{\text{source}}} \tag{15}$$

Two different definitions of the second law efficiency are used, based on the respective exergy supply rates

$$\eta_{\text{II,total}} = \frac{\dot{W}_{\text{net,out}}}{\dot{X}_{\text{source,total}}} \tag{16}$$

and

$$\eta_{\text{II,available}} = \frac{\dot{W}_{\text{net,out}}}{\dot{X}_{\text{source,available}}} \tag{17}$$

The values of $\eta_{\mathrm{II,available}}$ are larger than those of $\eta_{\mathrm{II,total}}$, because the available exergy rate is smaller than the total exergy rate at the same net power output.

Regenerative ORC

In case the temperature difference between the exit of the expander (state 2) and the exit of the pump (state 4) is at least 10 °C, an economizer with effectiveness ε may be used between expander and condenser. It transfers thermal energy as heat from the low-pressure side to the high-pressure side of the cycle. The specific enthalpy at the exit on the low pressure side of the economizer (state 2*) is

$$h_{2*} = h_2 - \varepsilon(h_2 - h_4) \tag{18}$$

The state at the high pressure outlet of the economizer (state 4*) has specific enthalpy

$$h_{4*} = h_4 + \varepsilon(h_2 - h_4) \tag{19}$$

The equation for the heat source fluid temperature at the preheater outlet is

$$T_{9b} = T_6 - \frac{\dot{m}_{\mathrm{ORC}}(h_1 - h_{4*})}{\dot{m}_{\mathrm{source}} c_{P,\mathrm{source}}} \geq T_{\mathrm{min,\ source}} \tag{20}$$

The corresponding mass flow rate of the heat sink fluid is

$$\dot{m}_{\mathrm{sink}} = \dot{m}_{\mathrm{ORC}} \frac{(h_{2,} - h_3)}{c_{P,\mathrm{sink}} \Delta T_{\mathrm{heat\ sink,max}}} \tag{21}$$

The temperature at the outlet of the heat sink for the ORC-working fluid becomes

$$T_{13b} = T_{12} - \frac{\dot{m}_{\mathrm{ORC}}(h_{2,} - h_{2*})}{\dot{m}_{\mathrm{sink}} c_{P,\mathrm{sink}}} \tag{22}$$

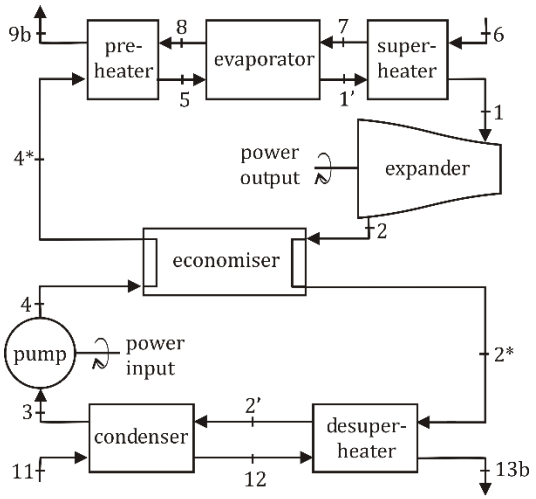

Figure 4: Setup of the regenerative ORC.

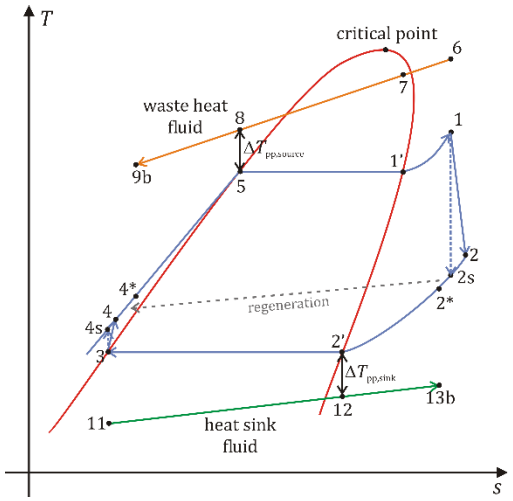

Figure 5: T-s-diagram for the regenerative ORC

Double source ORC

The double source ORC can be realized in two different ways. In the first case, the preheating of the ORC working fluid can be carried out first by a low temperature heat source, like the engine cooling water [10] (see Figure 6 and Figure 7). The preheating can either stop at a temperature lower than the ORC-fluid's saturation temperature (type 1 in this study) or go all the way to the saturation temperature. In the latter case (type 2), the high temperature heat source (exhaust gases) does not contribute to further preheating but performs the task of evaporating and eventually superheating the ORC working fluid. The states 4* and 5 are identical. One has the choice of basing the mass flow rate of the ORC-working fluid on either the heat transfer process with the low-temperature waste heat source or the high temperature source.

In the second case, the low temperature heat source is used for both preheating and evaporation of the ORC-working fluid [9] and the high temperature source is used for superheating only (see Figure 8 and Figure 9). This however limits the maximum pressure in the ORC-working fluid and thereby the pressure ratio in the ORC. However, a large pressure ratio is important for the net power output and thermal efficiency of a power cycle. In this case, the mass flow of the ORC working fluid is based on the heat exchange with the low temperature source.

The combined total exergy in both waste heat fluids is

$$\dot{X}_{\text{source,total}} = \dot{m}_{\text{source}} \left[c_{P,\text{source}}(T_6 - T_0) - T_0 \left(c_{P,\text{source}} \ln \frac{T_6}{T_0} - R \ln \frac{P_6}{P_0} \right) \right] + \dot{m}_{\text{low } T} \cdot c_{P,\text{source}} \left[T_{14} - T_0 - \ln \frac{T_{14}}{T_0} \right] \quad (23)$$

The mass flow rate of the heat sink fluid is in case of all double source ORCs

$$\dot{m}_{\text{sink}} = \dot{m}_{\text{ORC}} \frac{(h_2 - h_3)}{c_{P,\text{sink}} \Delta T_{\text{heat sink,max}}} \quad (24)$$

The final temperature of the heat sink fluid is

$$T_{13c} = T_{12} - \frac{\dot{m}_{\text{ORC}}(h_{2'} - h_2)}{\dot{m}_{\text{sink}} c_{P,\text{sink}}} \quad (25)$$

Type 1: Low temperature source for preheating of ORC working fluid only

Case A: The ORC mass flow is based on the heat exchange with the high temperature source. The ORC mass flow rate is calculated according to equation (8) and the specific enthalpy in state 4* is obtained by

$$h_{4^*} = h_4 + \frac{\dot{m}_{\text{source}} \cdot c_{P,\text{source}}(T_6 - T_8)}{h_1 - h_5} \quad (26)$$

The temperature drop in the low temperature waste heat fluid is then given by

$$\Delta T_{\text{low } T} = T_{14} - T_{15} = \frac{\dot{m}_{\text{ORC}}(h_{4*} - h_4)}{\dot{m}_{\text{low } T} \cdot c_{P,\text{low } T}} \quad (27)$$

In the optimization process, $\Delta T_{\text{low } T}$ is limited to 10 °C, which is a typical temperature drop in engine cooling water.

The temperature of the high temperature waste heat fluid is obtained by

$$T_{9c} = T_6 - \frac{\dot{m}_{\mathrm{ORC}}(h_1 - h_{4*})}{\dot{m}_{\mathrm{source}} c_{P,\mathrm{source}}} \geq T_{\mathrm{min,\ source}} \tag{28}$$

Case B: The ORC mass flow rate is based on the heat exchange with the low temperature source. The temperature in state 15 is set and later varied by the solver. The ORC mass flow is in this case

$$\dot{m}_{\mathrm{ORC}} = \dot{m}_{\mathrm{low}\ T} c_{P,\ \mathrm{low}\ T} \frac{(T_{14} - T_{15})}{(h_{4*} - h_4)} \tag{29}$$

The temperatures in states 7, 8 and 9c are then calculated in a different way than in case of the simple and regenerative ORC. The temperature in state 7 is

$$T_7 = T_6 - \frac{\dot{m}_{\mathrm{ORC}}(h_1 - h_{1,})}{\dot{m}_{\mathrm{source}} c_{P,\mathrm{source}}} \tag{30}$$

In state 8 it is

$$T_8 = T_7 - \frac{\dot{m}_{\mathrm{ORC}}(h_{1,} - h_5)}{\dot{m}_{\mathrm{source}} c_{P,\mathrm{source}}} \tag{31}$$

And in finally in state 9c

$$T_{9c} = T_8 - \frac{\dot{m}_{\mathrm{ORC}}(h_5 - h_{4*})}{\dot{m}_{\mathrm{source}} c_{P,\mathrm{source}}} \geq T_{\mathrm{min,\ source}} \tag{32}$$

The exergy supply due to the available temperature drop in exhaust gases and low temperature waste heat fluid is

$$\begin{aligned} \dot{X}_{\mathrm{source,available}} = \dot{m}_{\mathrm{source}} \left[c_{P,\mathrm{source}}(T_6 - T_{9c}) - T_0 \left(c_{P,\mathrm{source}} \ln \frac{T_6}{T_{9c}} - R \ln \frac{P_6}{P_{9c}} \right) \right] \\ + \dot{m}_{\mathrm{low}\ T} \cdot c_{P,\mathrm{source}} \left[T_{14} - T_{15} - \ln \frac{T_{14}}{T_{15}} \right] \end{aligned} \tag{33}$$

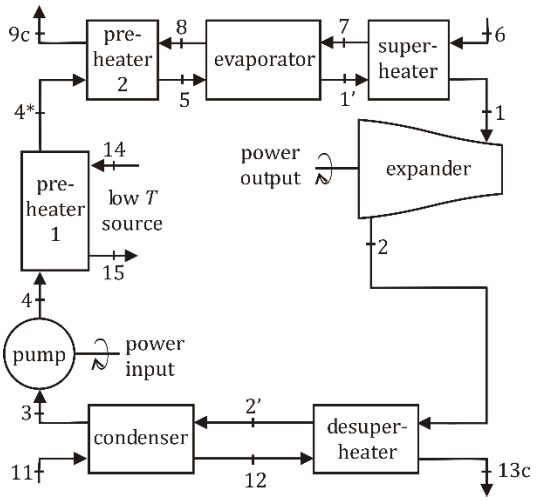

Figure 6: Double source ORC with two preheaters (type 1).

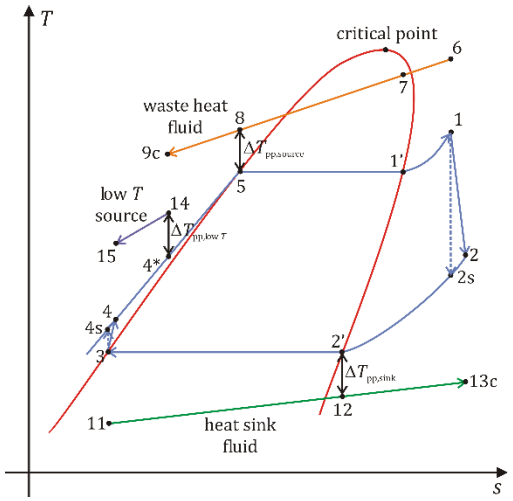

Figure 7: T-s-diagram for the double source ORC of type 1.

Type 2: Low temperature source for both preheating and evaporation of ORC working fluid

A value for the temperature drop $\Delta T_{\text{low }T}$ is set, which is smaller than the maximum allowed value $\Delta T_{\text{low }T,\,\text{max}}$. Based on this, the ORC mass flow rate is calculated based on the interaction with the low temperature waste heat fluid according to

$$\dot{m}_{\text{ORC}} = \dot{m}_{\text{low }T} c_{P,\,\text{low }T} \frac{(T_{14} - T_{16})}{(h_{1'} - h_4)} \tag{34}$$

The temperature in state 15, between preheater and evaporator on the low-temperature heat source side, is calculated with

$$T_{15} = T_{14} - \frac{\dot{m}_{\text{ORC}}(h_{1'} - h_5)}{\dot{m}_{\text{low }T} \cdot c_{P,\text{low }T}} \tag{35}$$

The temperature in the exhaust gases drops to a value according to equation (30).

The exergy supply due to the available temperature drop in exhaust gases and low temperature waste heat fluid is

$$\dot{X}_{\text{source,available}} = \dot{m}_{\text{source}} \left[c_{P,\text{source}} (T_6 - T_7) - T_0 \left(c_{P,\text{source}} \ln \frac{T_6}{T_7} - R \ln \frac{P_6}{P_7} \right) \right]$$
$$+ \dot{m}_{\text{low } T} \cdot c_{P,\text{source}} \left[T_{14} - T_{16} - \ln \frac{T_{14}}{T_{16}} \right] \quad (36)$$

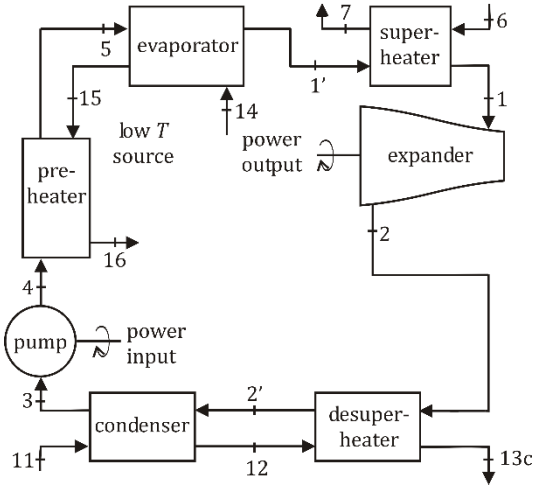

Figure 8: Double source ORC with preheating and evaporation by the low temperature heat source (type 2).

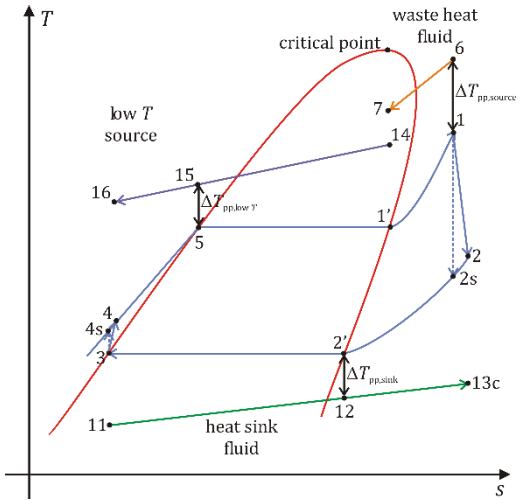

Figure 9: *T*-*s*-diagram for the double source ORC with preheating and evaporation by the low temperature heat source (type 2).

Optimization

The built in problem solver in Microsoft Excel® has been used to find the maximum net power output under certain given constraints. The GRG-non-linear solver was employed for this task. Table 2 shows the properties, which were varied by the solver for in the different models until a valid solution was found, which satisfied the various constraints.

Table 2: Properties varied by the solver in the different models

Model	**Variables**
Simple ORC	P_{max}, P_{min}, T_1, T_8
Regenerative ORC	P_{max}, P_{min}, T_1, T_8

Double source ORC, type 1, case A	$P_{\max}$, $P_{\min}$, T_1, T_{15}, T_8
Double source ORC, type 1, case B	$P_{\max}$, $P_{\min}$, T_1, T_{4*}
Double source ORC, type 2	$P_{\max}$, $P_{\min}$, T_1

The relevant constraints were

- $\Delta T_{\text{pp,source}} \geq \Delta T_{\text{pp,source,min}}$: keep minimum defined pinch point temperature difference at desired pinch point

- $T_6 - T_1 \geq \Delta T_{\text{pp,source,min}}$: keep the temperature difference between inlet of heat source fluid and outlet of working fluid at the evaporator also above or at the desired minimum value

- $T_{10} \geq T_{\min}$: heat source fluid must not be lower than a given minimum value

- $P_{\max} \leq P_{\text{cr, ORC}} - 250\ \text{kPa}$: keep the cycle subcritical and the pressure in a region of the phase diagram where the thermodynamic properties of the working fluid are known.

- $P_{\min} \geq P_{\text{sat}}(T_0 + \Delta T_{\text{condens.}})$: assure a high enough temperature during the condensation of the working fluid in order to obtain reasonable mass flows for the heat sink fluid.

- $x_2 \geq 90\%$: assure high enough quality at the end of the expansion process

As an additional constraint, the volumetric expansion ratio $r = v_2/v_1$ could be set to a certain value, like 5, for example, which is a typical ratio for volumetric expanders.

A number of other constraints had to be defined whose sole purpose was to obtain thermodynamically correct behaviour of all involved state variables while the solver was trying different solutions. These could be as simple as demanding $P_{\max} > P_{\min}$ because the solver has no preconception what these symbols and the values in the corresponding cells represent physically. Another such simple constraint

was that all efficiencies must be numbers between 0 and 1 and that the thermal efficiency cannot be larger than the Carnot-efficiency calculated with T_1 in kelvin as larger temperature value and T_0 in kelvin as lower temperature value.

Energy need for harbour transit

The necessary power for manoeuvring in and transiting harbours is

$$E_{\text{harbour}} = \dot{W}_{\text{harbour}} \Delta t_{\text{harbour}} \tag{37}$$

According to the numbers given in the data section above, 43.3 kWh are necessary.

The amount of energy, which can be recovered from the available waste heat and stored in the batteries during a return trip, is

$$E_{\text{recovered to battery}} = 2\eta_{\text{expander to battery}} \dot{W}_{\text{ORC,net.out}} \Delta t_{\text{cruising}} \tag{38}$$

The efficiency factor $\eta_{\text{expander to battery}}$ takes losses between expander and battery into account and has been set to 0.9 in the calculations. The factor 2 is necessary, because the ORC output power has been calculated per engine while the power needed and available for the different parts of the trip are given for the boast as a whole, driven by two engines with equal power at a time.

Based on these equations, it is also possible to calculate that each ORC-unit needs to deliver at least 131.1 kW in order to recover the necessary energy.

To easier evaluate if the necessary energy for the two harbour transits per return trip can be regenerated and how much a possible excess or deficit is, an energy recovery ratio has been defined by dividing equation (38) by equation (37)

$$r_{\text{recovery}} = \frac{\dot{W}_{\text{harbour}} \Delta t_{\text{harbour}}}{2\eta_{\text{expander to battery}} \dot{W}_{\text{ORC,net.out}} \Delta t_{\text{full ahead}}} 100\% \tag{39}$$

Values larger than 100 % will indicate that the necessary energy for electric harbour manoeuvring and transit can be recovered, while values smaller than 100 % will represent an energy deficit.

Choice of working fluids

Many different working fluids have been considered for ORCs connected to compression ignition engines. Ref. [2] gives a good overview over a number of different relevant publications and the working fluids used by their authors. For this study, a selection of different fluids was chosen where the criteria were low global warming potential (GWP), low ozone depletion potential (ODP) and low flammability, according to the ASHRAE classification (either 1 or 2L) [18]. Current EU regulation sets an upper limit on GWP for most applications of refrigerants to 150 from year 2022 on [19]. With respect to health and safety, low toxicity is preferable (A in the ASHRAE classification as opposed to B, which stands for higher toxicity) as the substance is to be used on a passenger vessel.

The choice fell onto the three hydrofluorolefins (HFO) R1234ze(Z), R1234ze(E), and R1234yf (all ASHRAE class A2L) and the hydrochlorofluoroolefin (HCFO) R1233zd(E), which has ASHRAE class A1. For comparison, the often used hydrofluorocarbon (HFC) R245fa (ASHRAE class B1) and ethanol were included in the study as well. R717 (ammonia) was part of the studied fluids as well due to having zero GWP and ODP. It is a working fluid often used in industrial and residential heat pump applications and even though it is in the higher toxicity class (B) with in the ASHRAE-scheme. It has a much higher critical pressure compared to the other fluids, but a critical temperature similar to that of the R1234ze-variants. It has shown a relatively small expansion ratio in the calculations and it is therefore an interesting candidate with respect to choice of expander technology. Ethanol and R717 have a ‘wet’ vapour part of the saturation curve (negative slope), while the aforementioned fluids have a ‘dry’ saturation curve.

Finally, water has been taken into the selection as well. BMW’s turbosteamer project was the motivation for this [20]. Water was used in a ORC-module to recover heat to electricity from the

exhaust gas from an internal combustion engine, while ethanol was used in a separate ORC recovering waste heat from a low temperature source. With a large enthalpy of vaporization, critical temperature close to that of the warmest heat source, and without any concerns regarding GWP, ODP, toxicity and flammability, water would be an interesting candidate for an ORC in the situation under investigation.

Table 3: Properties of the working fluids considered in the calculations. The critical properties and type of saturation curve were obtained with CoolProp. GWP (global warming potential) and ODP (ozone depletion potential) values were taken CoolProp-output as well. The ASHRAE classification was taken from the fluid-property pages in the CoolProp-online list of fluids for the respective substance [21].

Fluid	T_{crit} **/ °C**	P_{crit} **/ kPa**	**ASHRAE class**	**GWP**	**ODP**	**Saturation curve**
R1234ze(Z)	150.12	3533	A2L	~0	0	dry
R1234ze(E)	109.37	3636	A2L	6	0	dry
R1234yf	94.7	3382	A2L	4	0	dry
R1233zd(E)	166.45	3624	A1	~0	0	dry
R245fa	153.86	3651	B1	1030	0	dry
ethanol	241.56	6268	-	-	-	wet
ammonia (R717)	132.25	11333	B2L	0	0	wet
water (R718)	373.95	22064	-	-	-	wet

Calculations

For each of the three types of ORC, two sets of optimization calculations have been carried out. One set had no limit on the volumetric expansion ratio v_2/v_1, while the ratio was limited to 5 in the other

set. Volumetric expanders are both cheap and can be reasonably small, but they are limited to a certain expansion ratio. This usually lies between values of 4 – 5. The power output that can be achieved in the investigated scenario lies in power interval typical for scroll expanders [22].

Other limits were used in both sets of calculations. The maximum temperature in the ORC-working fluid (T_1) was limited to 300 °C. The maximum pressure, $P_{\max}$, was limited to the minimum of the working fluid's critical pressure minus 250 kPa and 4 MPa. The minimum pressure, $P_{\min}$, was limited to a value that guarantees at least 15 °C temperature difference to the temperature at the inlet of the heat sink fluid at the ORC's condenser outlet (state 3) or 50 kPa, whichever of both is the larger value. At the same time, the maximum allowed temperature increase in the heat sink fluid is set to 20°C. For ORC-working fluids with a wet saturation curve, the minimum necessary quality at the outlet of the expander was set to 90 %. All pinch point temperature differences must be at least 5 °C.

8.6 °C (annual average air temperature in Bergen in 2016 [23]) and 101.325 kPa were used as surroundings temperature and pressure. The heat sink fluid temperature at its inlet was set to 10 °C and the fluid itself assumed to be seawater with a specific heat capacity at constant pressure of 4.003 kJ/(kg·°C).

Results

Properties of the waste heat sources

Three source for waste heat have been considered in this investigation. These are the exhaust gas, the engine cooling water and the engine lubricant oil. The available thermal power and available exergy flow rate were calculated based on their thermal properties.

Exhaust gas

The mass flow of exhaust gas during the transit between harbours, when the engine is at 100% load, is based on the respective volume flow given in the OEM manual [13]. Its value is 3.25 m^3/s. A

temperature of 480 °C after the turbocharger exit is given in the manual and a backpressure of 70 mbar (gauge) over the surroundings pressure is assumed in order to have enough pressure in the gas to flow through the ORC-heat exchanger and the rest of the exhaust gas system. An average composition of the exhaust gas is neither given in the OEM manual nor was it possible to measure them on a boat running on these engines. A specified BSFC of 0.213 kg Diesel per kWh while the engine power is 900 kW gives a lambda of 1.96 [24]. Balancing a simple combustion equation with dry air and the corresponding amount of diesel fuel on the left hand side gives the composition given in Table 4 on the right hand side of the combustion equation.

Table 4: Composition of the exhaust gas

compound	Mass per kg fuel / kg	Mole fraction / %
N_2	22.0	82.2
CO_2	3.2	7.6
H_2O	1.2	7.0
O_2	0.96	3.1

The result is a mass flow of 1.61 kg/s. The specific gas constant of the exhaust gas is 0.290 kJ/(kg·K) and its specific heat capacity at constant pressure 1.139 kJ/(kg·K). The specific heat capacity ratio is k = 1.342.

A maximum temperature drop of 130 °C is allowed in order to ensure a high enough temperature in the exhaust gas when it enters the exhaust gas cleaning components. Therefore, 239 kW are available as heat if $T_{\min}$ in equation (10) is set to 350 °C and $T_{\max}$ to 480 °C. According to equation (15), the maximum available work potential of this heat is 138 kW.

Cooling liquid

The cooling liquid is a mixture of water with 40% anti-freeze-liquid. For the calculations, a 40 vol%-mixture of ethylene glycol with water is used. At full engine power, the volume flow of cooling liquid is 5.08 kg/s at 85°C and 300 kPa. The maximum allowed temperature drop in the cooler is 10°C. The maximum available heat is 190 kW, which has a work potential of 35 kW. The cooling liquid is considered as the low temperature waste heat fluid in the double source ORC.

Lubricant

The lubricant oil has a temperature between 78 C and 88 °C, similar to the cooling liquid. Unfortunately, a mass or volume flow is not known. Assuming a specific heat capacity of ca. 2 kJ/(kg·°C) and a maximum allowed temperature drop of 10 °C, the available specific heat is 20 kJ/kg lubricant. This is about 54% of the available specific heat of the cooling liquid, which has a specific heat capacity of 3.734 kJ/(kg·°C). Due to this lower amount of energy and corresponding available work potential, the lubricant is not considered as a heat source in the further analysis.

General overview

Table 5 and Table 6 contain the most important results for all ORC models and working fluids. Table 5 shows the results for unconstrained expansion.

Table 5: Most important results for all ORC-types for unconstrained expansion.

ORC-type	Fluid	net power output / kW	recovery factor	thermal efficiency	exergy efficiency	expansion ratio	pressure ratio	ORC mass flow / kg/s	Volume flow at exp. outlet / L/s
simple ORC	R1234ze(Z)	45.3	34.5 %	19.0 %	32.2 %	16.6	17.4	0.557	93.8

	R1234ze(E)	33.6	25.6 %	14.1 %	23.9 %	6.41	6.59	0.680	40.3
	R1234yf	28.4	21.6 %	11.9 %	20.2 %	4.47	4.50	0.779	32.3
	R1233zd(E)	47.5	36.2 %	19.9 %	33.8 %	23.4	24.3	0.595	120
	R245fa	43.4	33.1 %	18.2 %	30.9 %	21.1	20.9	0.643	100
	ethanol	57.7	43.9 %	24.2 %	41.0 %	61.2	80.0	0.188	260
	ammonia	34.5	26.3 %	14.5 %	24.5 %	2.79	3.45	0.132	24.8
	water	53.9	41.0 %	22.6 %	38.3 %	24.0	41.2	0.0891	260
regenerative ORC	R1234ze(Z)	62.0	47.2 %	26.0 %	44.1 %	13.8	14.7	0.735	115
	R1234ze(E)	46.8	35.6 %	19.6 %	33.3 %	5.41	5.59	0.984	52.2
	R1234yf	38.7	29.5 %	16.2 %	27.5 %	3.81	3.81	1.20	42.4
	R1233zd(E)	64.3	48.9 %	26.9 %	45.7 %	19.3	20.4	0.789	143
	R245fa	61.3	46.7 %	25.7 %	43.6 %	17.2	18.2	0.775	126
	ethanol	61.0	46.5 %	25.6 %	43.4 %	61.2	80.0	0.199	275
	ammonia	35.3	26.9 %	14.8 %	25.1 %	2.50	3.05	0.171	25.2
	water	20.9	15.9 %	8.8 %	14.9 %	2.81	3.72	0.0937	312
double source ORC, type 1, case A	R1234ze(Z)	55.3	42.1 %	18.6 %	36.1 %	16.7	15.5	0.917	112
	R1234ze(E)	45.7	34.8 %	13.3 %	28.1 %	6.43	5.60	1.53	56.3
	R1234yf	43.1	32.8 %	10.6 %	24.7 %	4.62	3.68	2.37	54.1

	R1233zd(E)	58.0	44.2 %	19.5 %	37.9 %	24.1	21.5	0.983	142
	R245fa	55.1	42.0 %	17.8 %	35.4 %	22.4	18.4	1.09	125
	ethanol	60.0	45.7 %	24.2 %	42.0 %	61.2	80.0	0.195	270
	ammonia	39.9	30.4 %	14.5 %	26.9 %	2.79	3.45	0.152	28.7
	water	62.1	47.3 %	24.7 %	43.3 %	48.3	94.6	0.0878	1160
double source ORC, type 1, case B	R1234ze(Z)	55.3	42.1 %	18.6 %	36.1 %	16.7	15.5	0.914	112
	R1234ze(E)	44.6	34.0 %	12.8 %	27.3 %	5.92	5.15	1.59	57.1
	R1234yf	43.1	32.8 %	10.6 %	24.7 %	4.62	3.68	2.37	54.1
	R1233zd(E)	57.2	43.6 %	19.1 %	37.3 %	22.2	19.8	1.00	143
	R245fa	54.0	41.1 %	17.2 %	34.6 %	19.7	16.1	1.14	126
	ethanol	58.8	44.8 %	23.9 %	41.4 %	56.6	74.0	0.193	270
	ammonia	38.5	29.3 %	14.1 %	26.0 %	2.70	3.31	0.151	28.8
	water	58.7	44.7 %	30.6 %	51.7 %	200	400	0.0693	814
double source ORC, type 2	R1234ze(Z)	39.6	30.1 %	9.85 %	24.1 %	3.81	4.05	0.806	174
	R1234ze(E)	40.5	30.8 %	9.46 %	22.6 %	3.35	3.51	0.995	72.6
	R1234yf	40.1	30.5 %	9.36 %	22.4 %	3.19	3.30	1.16	56.6
	R1233zd(E)	37.7	28.7 %	9.68 %	24.0 %	3.96	4.22	0.851	220
	R245fa	37.8	28.7 %	9.14 %	22.1 %	4.20	4.43	0.841	187

	ethanol	33.4	25.4 %	12.0 %	36.1 %	6.36	7.36	0.195	1697
	ammonia	39.6	30.1 %	13.1 %	36.8 %	2.49	3.01	0.167	32.6
	water	18.8	14.3 %	8.4 %	31.2 %	2.50	3.18	0.078	1617

Table 6 contains the results for the cases, where the expansion ratio was limited to a maximum value of 5.

Table 6: Most important results for all ORC-types with expansion ratio limited to a value of 5.

ORC-type		net power output / kW	recovery factor	thermal efficiency	exergy efficiency	expansion ratio	pressure ratio	ORC mass flow / kg/s	Volume flow at exp. outlet / L/s
simple ORC	R1234ze(Z)	29.8	22.7 %	12.5 %	21.2 %	5.00	5.07	0.766	74.8
	R1234ze(E)	30.1	22.9 %	12.6 %	21.4 %	5.00	5.03	0.786	40.8
	R1234yf	28.4	21.6 %	11.9 %	20.2 %	4.47	4.50	0.779	32.3
	R1233zd(E)	29.0	22.1 %	12.1 %	20.6 %	5.00	5.01	0.881	84.9
	R245fa	27.3	20.8 %	11.4 %	19.4 %	5.00	4.95	0.919	87.7
	ethanol	29.4	22.4 %	12.3 %	20.9 %	5.00	5.34	0.233	26.6
	ammonia	34.5	26.3 %	14.5 %	24.5 %	2.79	3.45	0.132	24.8

	water	34.8	26.5 %	14.6 %	24.8 %	5.00	6.80	0.102	37.5
regenerative ORC	R1234ze(Z)	44.0	33.5 %	18.5 %	31.3 %	5.00	5.04	0.925	49.1
	R1234ze(E)	45.0	34.3 %	18.9 %	32.0 %	5.00	5.14	1.01	48.8
	R1234yf	38.7	29.5 %	16.2 %	27.5 %	3.81	3.81	1.20	42.4
	R1233zd(E)	43.5	33.1 %	18.2 %	30.9 %	5.00	5.01	1.02	47.5
	R245fa	40.7	31.0 %	17.1 %	28.9 %	5.00	4.97	1.03	44.2
	ethanol	34.4	26.2 %	14.4 %	24.4 %	5.00	5.48	0.252	49.4
	ammonia	35.3	26.9 %	14.8 %	25.1 %	2.50	3.05	0.171	25.2
	water	26.8	20.4 %	11.3 %	19.1 %	3.86	5.55	0.091	437
double source ORC, type 1, case A	R1234ze(Z)	32.3	24.6 %	11.5 %	21.9 %	4.79	4.33	1.26	76.0
	R1234ze(E)	23.6	17.9 %	8.1 %	15.1 %	2.66	2.52	1.480	51.2
	R1234yf	37.7	28.7 %	10.2 %	22.5 %	3.47	3.29	1.65	51.0

	R1233zd(E)	38.5	29.4 %	11.9 %	24.4 %	5.00	4.89	1.45	157
	R245fa	37.9	28.9 %	11.3 %	23.6 %	5.00	4.78	1.50	138
	ethanol	27.7	21.1 %	11.2 %	19.4 %	5.00	5.66	0.186	337
	ammonia	39.9	30.4 %	14.5 %	26.9 %	2.79	3.45	0.152	28.7
	water	33.4	25.4 %	13.3 %	23.3 %	5.00	7.63	0.087	1506
double source ORC, type 1, case B	R1234ze(Z)	34.3	26.1 %	12.4 %	23.0 %	5.00	4.83	0.973	64.0
	R1234ze(E)	42.2	32.2 %	12.0 %	25.7 %	4.98	4.48	1.60	58.1
	R1234yf	43.1	32.8 %	10.6 %	24.7 %	4.62	3.68	2.37	54.1
	R1233zd(E)	38.5	29.4 %	11.9 %	24.4 %	5.00	4.89	1.45	157
	R245fa	37.9	28.9 %	11.3 %	23.6 %	5.00	4.78	1.50	138
	ethanol	27.1	20.6 %	11.2 %	19.1 %	5.00	5.66	0.182	329
	ammonia	39.9	30.4 %	14.5 %	26.8 %	2.79	3.45	0.152	28.7

	water	33.4	25.4 %	13.3 %	23.3 %	5.00	7.63	0.0871	1506
double source ORC, type 2	R1234ze(Z)	39.6	30.1 %	9.85 %	24.1 %	3.81	4.05	0.806	174
	R1234ze(E)	40.5	30.8 %	9.46 %	22.6 %	3.35	3.51	0.995	72.6
	R1234yf	40.1	30.5 %	9.36 %	22.4 %	3.19	3.30	1.16	56.6
	R1233zd(E)	37.7	28.7 %	9.68 %	24.0 %	3.96	4.22	0.851	220
	R245fa	37.8	28.7 %	9.14 %	22.1 %	4.20	4.43	0.841	187
	ethanol	29.7	22.6 %	10.7 %	31.9 %	5.00	5.68	0.198	1357
	ammonia	39.6	30.1 %	13.1 %	36.8 %	2.49	3.01	0.167	32.6
	water	18.8	14.3 %	8.35 %	31.2 %	2.50	3.18	0.078	1617

Power output in the different ORC-models

Simple ORC

Figure 10 shows the achievable power output as obtained by the optimization. Without constraints on the volumetric expansion ratio, up to 57 kW net power can be achieved with ethanol as the working fluid. The different refrigerants (HFO, R1233zd(E) and R245fa) achieve only 28-47 kW, while ammonia and water can deliver 34.5 kW and 54 kW respectively. However, this is much less than the necessary

131 kW calculates above. The obtainable power with constrained expansion is much more even between the different fluids with ca. 30 kW on the average. The corresponding recovery factors are shown in Figure 11.

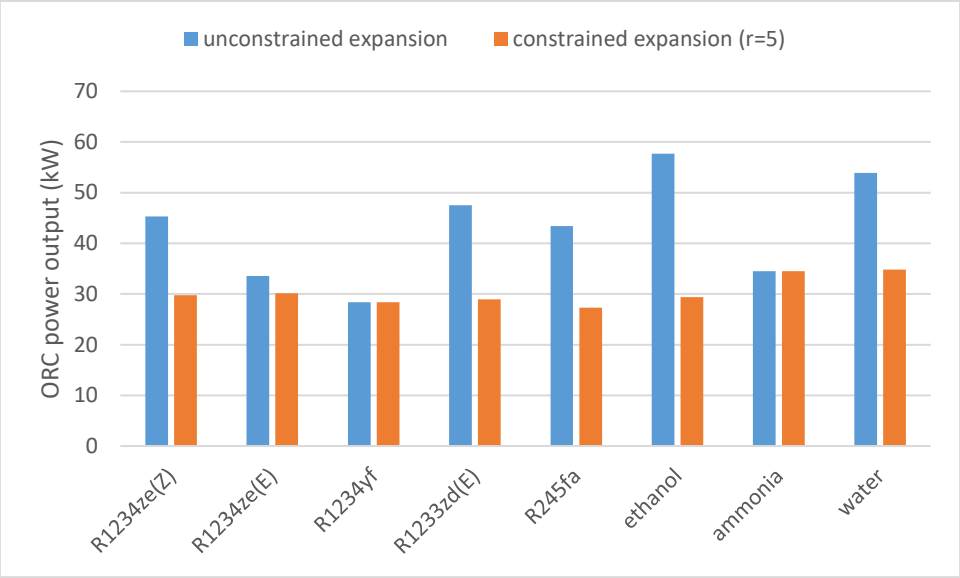

Figure 10: net power output for the simple ORC for both unconstrained and constrained expansion.

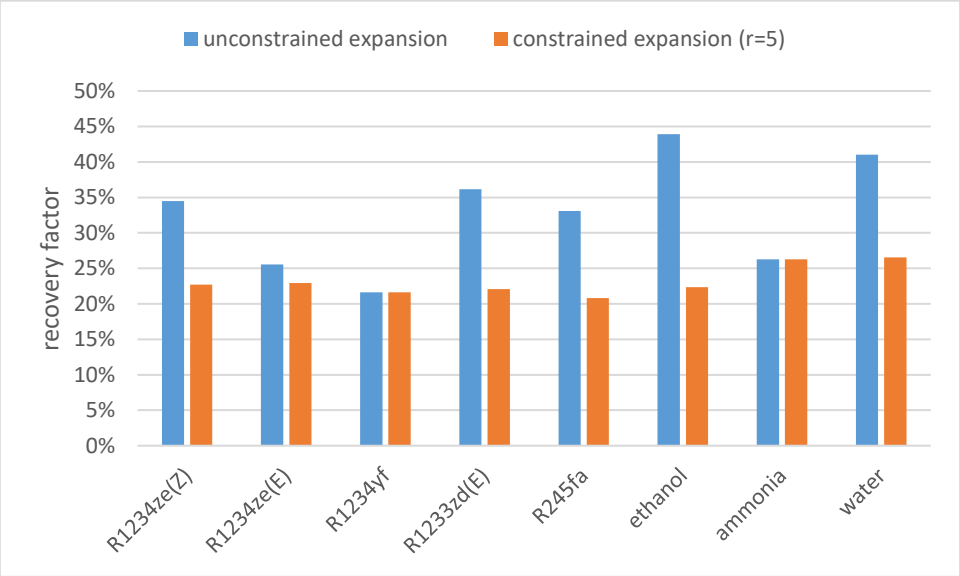

Figure 11: Recovery factor for the simple ORC for both unconstrained and constrained expansion.

Without constraint on the expansion of the ORC-fluid, a maximum of 43.9 % of the necessary energy for electric harbour manoeuvring and transit can be recovered by the best performing fluid, while between 21-27% of the necessary energy can be recovered only when the expansion is constrained to

a volumetric ratio of 5. Tables 5 and 6 show, that the thermal efficiencies lie in the range from 12-24% (the latter for ethanol) for the unconstrained expansion and 11-14.6% for the limited expansion process. The corresponding exergy efficiencies lie between 20% and 41% for the unconstrained expansion and 20% to 25% for the constrained expansion process. Another interesting property to look at is the volume flow of the working fluid at the expander outlet. The smallest values are obtained for ammonia (24.8 L/s) and R1234yf (32.2 L/s) regardless of a constraint on the expansion ratio. However, ammonia has the larger recovery factor of both fluids in the case of constrained expansion: 26.3% compared to 21.6% for R1234yf. When no limit is set on the volumetric expansion ratio, R1233zd(E) performs better compared to ammonia, with a recovery factor of 36.2% compared to 26.3%.

Regenerative ORC

More fluids perform better when internal regeneration of thermal energy is used. Compared to the simple ORC, four instead of one working fluid achieve more than 45 % of what needs to be recovered in energy when the expansion is not constrained (see Figure 12). These are ethanol, R1234ze(Z), R1233zd(E) and R245fa. R1234ze(Z) has the lowest expansion ratio of these five fluids (13.8) and also the lowest volume flow at the expander outlet (115 L/s)in unconstrained expansion. Water is not a useful working fluid in this type of ORC; it has the lowest recovery factor of all fluids.

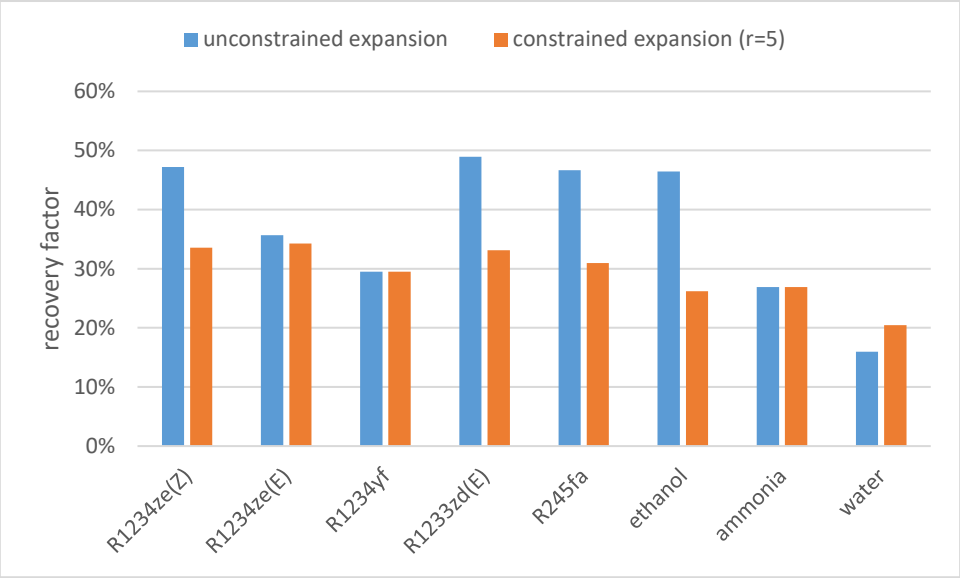

Figure 12: Recovery factor for the regenerative ORC for both unconstrained and constrained expansion.

Overall, the recovery ratio increases by almost 50% on average for the three HFOs, R1233zd(E) and R245fa when the expansion is constrained to r= 5. The values for ethanol and ammonia hardly change compared to the simple ORC. The energy recovery is largest for R1234ze(Z), R1234ze(E) and R1233zd(E) (ca. 33% recovery factor). Several other properties of these fluids have quite value, like the thermal efficiency (ca. 18%), exergy efficiency (ca. 31%), and volume flow at expander outlet (ca. 49 L/s) and ORC-fluid mass flow of around 1 kg/s.

Double source ORC, type 1

The maximum thermal power available is 239 kW in both the simple and regenerative ORC as only one heat source (exhaust gas; high temperature) is used in these models. When combined with the available thermal power in the engine coolant, this maximum available thermal power increases to 428 kW. However, the ORC-working fluid can recover only a part of it. The reason is that the energy recovery from the engine coolant is limited to the preheating of the liquid ORC-fluid coming from the pump. The process stops when either the ORC-fluid is at its boiling point at the given maximum pressure or when its temperature is at 80 °C ($T_{14} - \Delta T_{\mathrm{pp,\,low}\ T,\,\mathrm{min}}$) while still in the liquid phase. In the

first case, states 4* and 5 are the same, while $T_{4*} < T_5$ in the second case. Figure 13 shows the amount of heat transferred to the ORC working fluid.

Two different cases are investigated for this type of ORC. In case A, the ORC-mass flow is defined by interaction with exhaust gas according to equation (8), while the interaction with the low temperature engine water is used to calculate the ORC-mass flow in case B according to equation (29).

In general, the differences in results for the recovery factor (and other properties) between cases A and B a small for both unconstrained and constrained expansion. Figure 13 shows the fraction of absorbed heat by the ORC-fluid mass flow for case A.

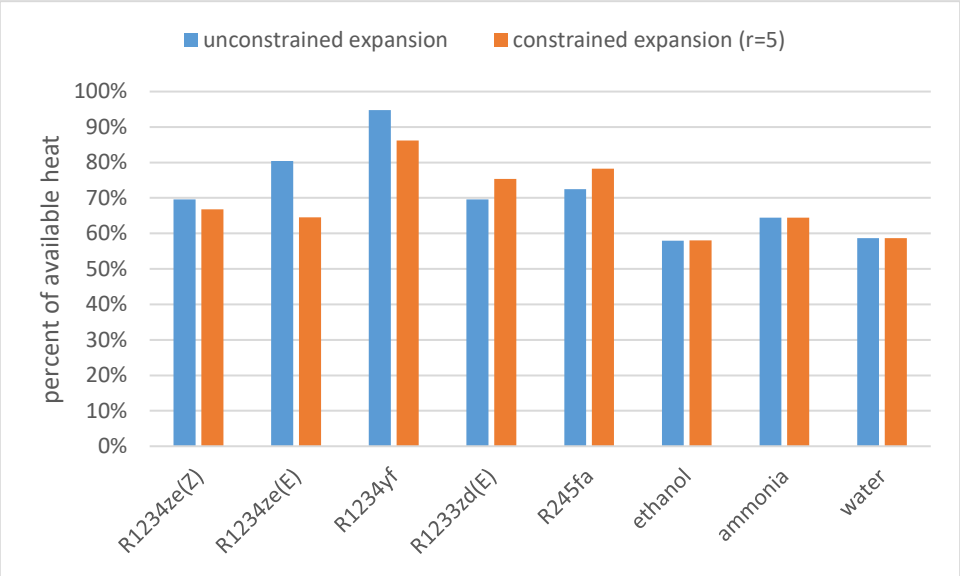

Figure 13: Percentage of the available heat absorbed by the ORC-fluid for both types of expansion process in case A. The maximum available thermal power is 428 kW for the double-source ORCs.

The fraction of absorbed to available heat varies between 58% for ethanol and 95% for R1234yf for the unconstrained expansion and between 58% and 86% for the same fluids for the constrained expansion process. With regard to energy recovery, ethanol and water perform best with ca. 45% recovery factor, corresponding to ca. 60 kW of recovered power. Among the HFOs, R1233zd(E) and R145fa, the best fluid is R1233zd(E) with 44% recovery factor, followed by R1234ze(Z) with 41%. R1234yf is the weakest one with only 33%.

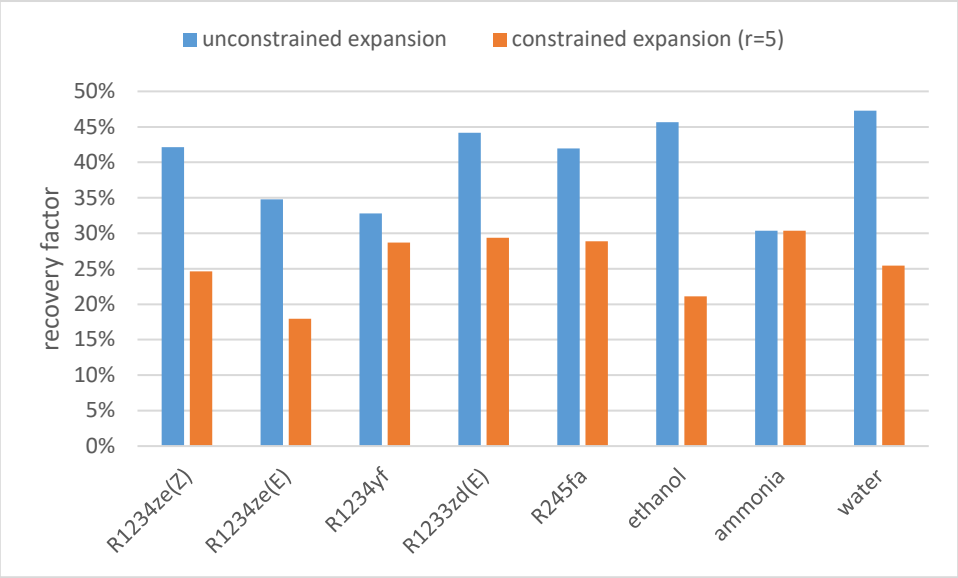

Figure 14: Recovery factor for the two expansion processes for the double-source ORC with ORC-mass flow defined by the heat transfer from the exhaust gas.

It is only possible to achieve more than 45% of the necessary energy recovery with two of the selected fluids in case of the unrestricted expansion process (ethanol and water; see Figure 14). For the constrained expansion, less energy is recoverable with most of the fluids than in the regenerative ORC. The maximum is 30%.

In case B, the corresponding recovery ratios are almost the same as in case A. Exceptions are R1234ze(E) and R1234yf, which have higher recovery factors than in case A for the constrained expansion. Here, R1234yf is the best candidate among the HFOs, R1233zd(E) and R245fa. It has a recovery factor of 33%, closely followed by R1234ze(Z) (32%) and R1233zd(E) (29.5%). The latter also has the largest volume flow at the expander outlet with 76 L/s (case A) and 64 L/s (case B).

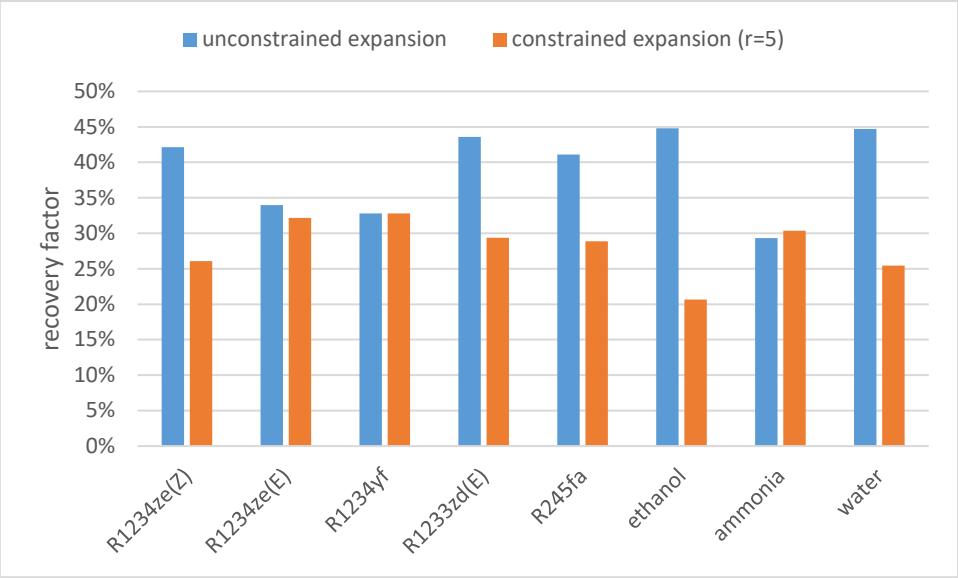

Figure 15: Recovery ratio for the ORCs of type 1, case B.

Overall, thermal efficiencies and exergy efficiencies are lower for the HFOs and R1233zd(E) compared to the regenerative ORC and more on the level of the simple ORC.

Type 2: low temperature fluid used for both preheating and evaporation of ORC fluid

For comparison, both thermal power absorbed as heat and recovery factor are shown for the double source ORC-model, where the ORC-mass flow rate is defined by the mass flow and enthalpy change low temperature waste heat source.

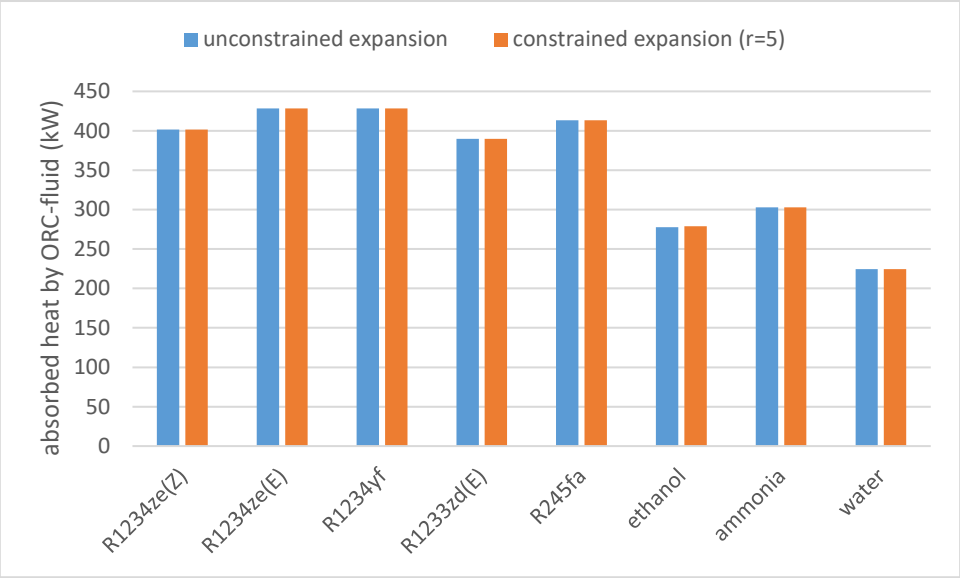

Figure 16: Absorbed thermal power as heat by the ORC-fluid for both types of expansion process. The maximum available thermal power is 428 kW for the double-source ORC with ORC-mass flow defined by the heat transfer from engine cooling water.

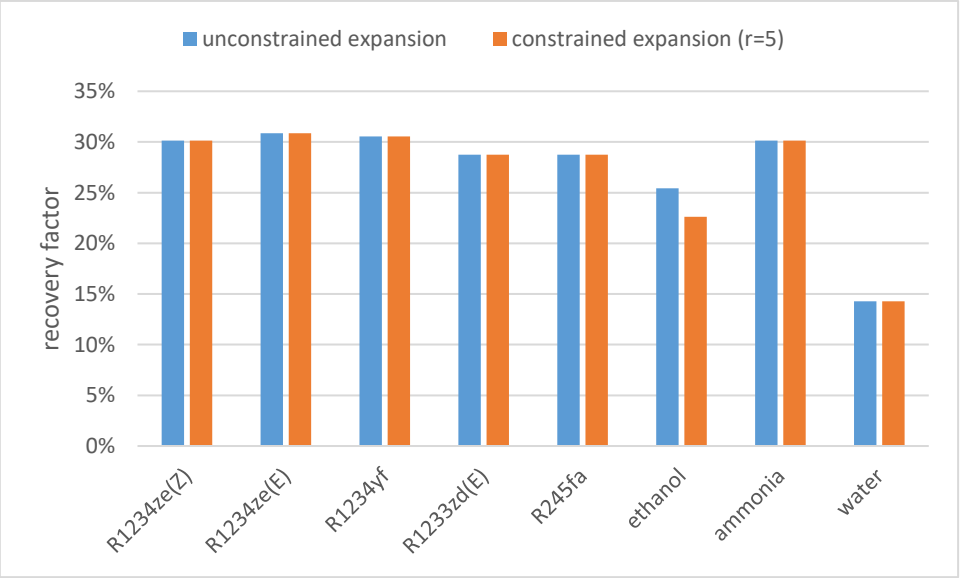

Figure 17: Recovery factor for the two expansion processes for the double-source ORC with ORC-mass flow defined by the heat transfer from the engine cooling water.

As mentioned before, using the engine cooling liquid for both preheating and evaporation of the ORC working fluid limits the pressure ratio to a value corresponding to the saturation pressure at a temperature below 85 °C. This leads to almost identical results for the HFOs, with R1233zd(E), R245fa and ammonia close behind. 40 kW ORC net output power can be achieved with the HFOs,

corresponding to 30% of the necessary energy recovery for electric propulsion. Of these six substances, the lowest volume flow at the expander outlet is noted for R1234yf (57 L/s), R1234ze(E) (73 L/s) and R1234ze(Z) (174 L/s).

Even when the expansion ratio was limited to a value of 5, it was only ethanol, which exceeded this value in unconstrained expansion and was limit to this value in the constrained expansion calculations. The other substances has clearly smaller values of 3.2 – 3.8 (HFOs) and approximately 4 for both 1233zd(E) and R245fa. Even though water had one of the smallest expansion ratios, the actual volume flows at both inlet and outlet of the expander are very large with 648 L/s and 1617 L/s. Ethanol has values on a similar scale with 267 L/s and 1697 L/s.

Due to their larger volume flows, which also requires larger expanders, both water and ethanol are not appropriate as candidates for a double source ORCs with restrictions set by the space they have to be integrated into together with battery and charger.

Discussion

Among the results, a regenerative ORC appears to be the best suited solution for recovering energy from the exhaust gases with respect to the power that can be recovered and the limited space such an appliance needs to be integrated into. The HFOs considered in this work have performed well among the studied fluids and R1234ze(Z) appears to be the most promising candidate among them.

However, it is not possible to recover enough energy from the available waste heat sources on board by means of different types of ORC with or without constrained expansion. This is mainly due to the short transit time at cruising speed compared to the time necessary for manoeuvring and harbour transit. Among the different ORC-types, the regenerative cycle has given the best results with respect to the potential net ORC output power achievable with the different fluid types. Figure 18 shows how long the necessary transit time at cruising speed needs to be in order to recover the necessary energy.

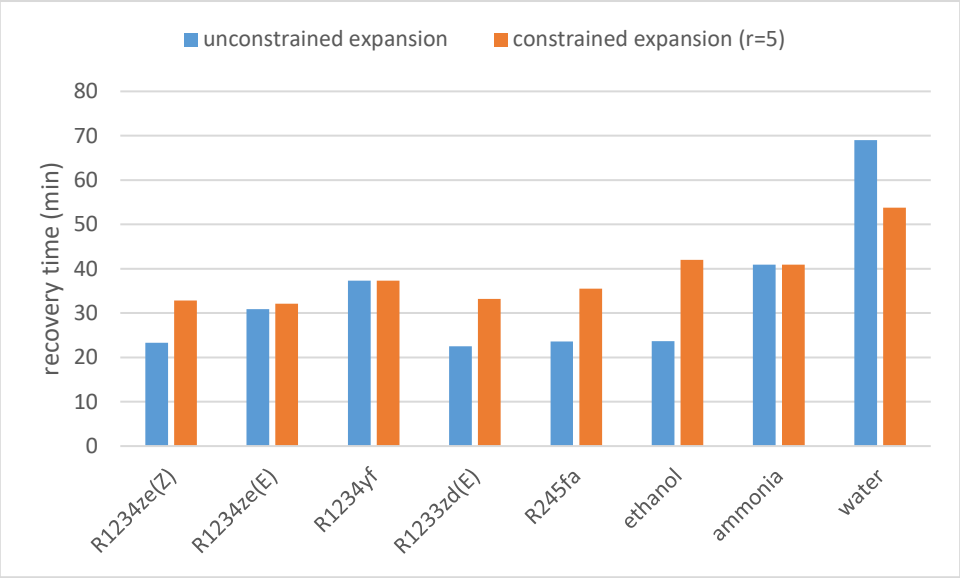

Figure 18: Necessary time in minutes to recover the energy needed for 13 min of harbour transit and manoeuvring when using a regenerative ORC.

The time lies between 22 and 37 minutes for most of the fluids for the unconstrained and constrained expansion, respectively. For R1234yf, these times are actually equal. These are time intervals that are typical for the time between stops of fast passenger boats that travel longer distances along the Norwegian west coast. At the stops along these routes, the time for manoeuvring and transit through harbour zones is often shorter than in Bergen, for example.

Based on equations (37) and (38), a ratio between necessary cruising time to time spent on manoeuvring and harbour transit can be derived based on the properties $\dot{W}_{\text{harbour}}$, $\dot{W}_{\text{ORC,net,out}}$, and $\eta_{\text{expander to battery}}$.It has to be exceeded in order to be able to recover enough energy for electric propulsion during the time.

$$\left(\frac{\Delta t_{\text{cruising}}}{\Delta t_{\text{harbour}}}\right)_{\text{min}} = \frac{\dot{W}_{\text{harbour}}}{\eta_{\text{expander to battery}} \dot{W}_{\text{ORC,net.out}}} \tag{40}$$

For the case under investigation, this value is 7.4, while the actual ratio of these times for a single crossing is 1.8 for the harbour of Askøy, and 0.55 for the harbour of Bergen. For a $\Delta t_{\text{harbour}}$ of 3 min, which would be a typical average value for the longer routes, the necessary cruising time is 22.2 min, which would be achievable in many places on the longer inner coastal routes.

The amount of energy to be stored lies around 50 kWh in the studied scenario. This is a typical size in recent fully electric passenger vehicle (EPV). These should be easy to retrofit on board an existing vessel. However, one has to consider the frequency of charging and discharging cycles, which will be much higher than on a normal EPV. A larger battery capacity could be considered, that is pre-charged to a certain amount before the first voyage of the day.

Another aspect to be considered is the actual size and weight of the components of the ORC-unit. Compact ORC-units have been constructed for Diesel-engines in passenger cars (BMW turbosteamer [20]) and cargo trucks (for example Cummins-Peterbilt [25]), but these recovered a much smaller power from the available waste heat sources. In order to recover thermal power on the order of around 30 kW, much larger heat exchangers are needed than in the road vehicle solutions, especially when a third heat exchanger in a regenerative ORC or a double-source ORC is needed.

In this context, the actual volume flow at the outlet of the expander is of interest. In Figure 19, the volume flow interval between inlet (bottom of each vertical line) and outlet (top of each line) is shown in litres per second for the constrained expansion in a regenerative ORC. The values are quite similar for most of the fluids and are mainly between 10 and 50 litres per second. Water has by far the largest volume flows, while ammonia has the smallest ones of all studied fluids.

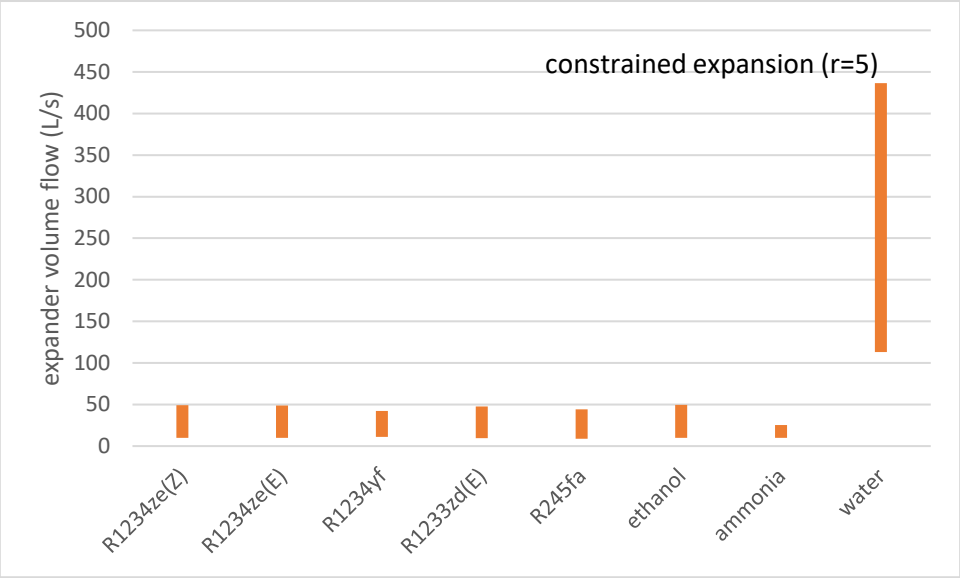

Figure 19: Expander volume flow in litres per second at inlet (bottom value) and outlet (top value) for a constrained expansion process in a regenerative ORC.

Since the recovered energy during full ahead transit between stopovers is not enough for electric propulsion, the question arises if charging with land based power can compensate for the difference between energy need and available energy from on-board recovery. As there are only 25 min 30 s per stopover and an automated system needs some time to connect and disconnect (10 s assumed for both connect and disconnect), only 2 min 10 s are available for charging during the shortest stopovers. Depending on type of ORC and working fluid, between 257 kW and 418 kW charging power are necessary. Such systems are commercially available and add to the investment cost of the necessary modifications of the vessel to house an ORC on each engine and the accompanying generators, chargers and battery.

Another measure to reduce local emissions is either mooring with lines or by means of an electromagnetic system instead of thrusting to keep the vessel stationary during the short stopovers. Mooring with lines is considered to take too much time and the persons handling the mooring lines need to be certified for this. Electromagnetic mooring systems exist and could guarantee quick mooring while being part of an eventual land based charging system.

Even if a Diesel-ORC-electric solution is both technically and economically possible, it could be outdated as soon as decision makers ask for zero-(greenhouse gas)-emission vessels, for example fully electric or based on hydrogen as fuel, in the next round of public tenders for public transport.

This study has not investigated the economic aspects of adding an ORC and the additional components for a hybrid powertrain to an existing Diesel-powered fast passenger ferry. This is the subject of further work. Two aspects that are often forgotten in purely thermodynamic investigations are rules and regulations concerning the use of technical fluids in certain environments and simple price comparisons. Although traded as a replacement for R134a, there are relatively few reports so far on the use of HFOs of the R1234ze-type in maritime environments. R1234yf is already in use in automotive applications. With the ASHRAE-class being A2L for the three R1234-fluids used in this investigation, it may be difficult and technically challenging to implement their use into existing legislative frameworks, which require low flammability corresponding to the A1 class of fluids, for example. In addition, their price is still very high with US $110 – 150 per kg R1234yf and R1234ze(E) costing about a third of this [26]. The price for a kg of ammonia is around US $1 per kg. However, regarding the scale of the necessary components, the amount and therefore cost of working fluid is not expected to have a big impact on the total cost of the ORC module in the hybrid powertrain. Furthermore, an increased demand for HFOs may be expected due to the phasing out of the HFCs they are to replace. This should lead to an increase in production capacity and therefore lower prices.

Conclusions and further work

The transit time for crossing the fjord between Bergen and Askøy is too short for recovering enough energy from the exhaust gas and engine cooling liquid in order to allow for electric propulsion and manoeuvring in the harbour in Bergen and Askøy. However, this technology may still be interesting for the routes with longer distances between stops and shorter time with electric propulsion, which stretch from Bergen into the districts along the coast in Western Norway. This includes both retrofitting

as well as the design of a newer generation of fast passenger boats with propulsion based on (bio-)Diesel as fuel.

As a lookout to further work, it would be interesting to investigate scenarios where hydrogen and fully battery powered fast passenger boats are too expensive, and fast passenger boats running on biodiesel with ORC and battery already taken into account at design stage are an alternative. Considering a higher engine load to fill batteries and the corresponding higher fuel consumption and emissions could be compared to scenarios where the three investigated ORC-types in this work are used instead.

Further work will cover a comparison of the energy recovery potential o fa turbogenerator in the exhaust gas flow, a comparison of the space ORC and turbogenerator systems and batteries will need and a comparison of the actual costs of retrofitting such components to existing propulsion systems.

Acknowledgements

The authors are grateful to the local MTU engine distributor Bostek for getting insight into the engine data of MS Teisten.

References

[1] Statistics Norway. *Public Transport 2016*. Available at: https://www.ssb.no/en/transport-og-reiseliv/statistikker/kolltrans/aar, accessed online: 1st December 2017.

[2] V. Chintala, S. Kumar, J.K. Pandey. A technical review on waste heat recovery from compression ignition engines using organic Rankine cycle. Renewable and Sustainable Energy Reviews. 81 (2018) 493-509.

[3] A. Nour Eddine, D. Chalet, X. Faure, L. Aixala, P. Chessé. Optimization and characterization of a thermoelectric generator prototype for marine engine application. Energy. 143 (2018) 682-95.

[4] R. Zhao, W. Zhuge, Y. Zhang, Y. Yin, Z. Chen, Z. Li. Parametric study of power turbine for diesel engine waste heat recovery. Applied Thermal Engineering. 67 (2014) 308-19.

[5] R. Pili, A. Romagnoli, K. Kamossa, A. Schuster, H. Spliethoff, C. Wieland. Organic Rankine Cycles (ORC) for mobile applications – Economic feasibility in different transportation sectors. Applied Energy. 204 (2017) 1188-97.

[6] G. Shu, P. Liu, H. Tian, X. Wang, D. Jing. Operational profile based thermal-economic analysis on an Organic Rankine cycle using for harvesting marine engine's exhaust waste heat. Energy Conversion and Management. 146 (2017) 107-23.

[7] F. Kyriakidis, K. Sørensen, S. Singh, T. Condra. Modeling and optimization of integrated exhaust gas recirculation and multi-stage waste heat recovery in marine engines. Energy Conversion and Management. 151 (2017) 286-95.

[8] C. Sellers. Field operation of a 125kW ORC with ship engine jacket water. Energy Procedia. 129 (2017) 495-502.

[9] M.-H. Yang, R.-H. Yeh. Thermo-economic optimization of an organic Rankine cycle system for large marine diesel engine waste heat recovery. Energy. 82 (2015) 256-68.

[10] J. Song, Y. Song, C.-w. Gu. Thermodynamic analysis and performance optimization of an Organic Rankine Cycle (ORC) waste heat recovery system for marine diesel engines. Energy. 82 (2015) 976-85.

[11] M. Zhao, M. Wei, P. Song, Z. Liu, G. Tian. Performance evaluation of a diesel engine integrated with ORC system. Applied Thermal Engineering. 115 (2017) 221-8.

[12] R. Scaccabarozzi, M. Tavano, C.M. Invernizzi, E. Martelli. Thermodynamic Optimization of heat recovery ORCs for heavy duty Internal Combustion Engine: pure fluids vs. zeotropic mixtures. Energy Procedia. 129 (2017) 168-75.

[13] MTU. *Technical Sales Document 10V2000M72* Available at: http://boatdiesel.com/Engines/MTU/MTU.cfm, accessed online: 1st december 2017.

[14] C.N. Michos, S. Lion, I. Vlaskos, R. Taccani. Analysis of the backpressure effect of an Organic Rankine Cycle (ORC) evaporator on the exhaust line of a turbocharged heavy duty diesel power generator for marine applications. Energy Conversion and Management. 132 (2017) 347-60.

[15] T. Tveiten Lewis. Hybridization of High-Speed Passenger Vessels [master thesis]. Bergen: University of Bergen; 2016.

[16] D. Mikielewicz, J. Mikielewicz. Analytical method for calculation of heat source temperature drop for the Organic Rankine Cycle application. Applied Thermal Engineering. 63 (2014) 541-50.

[17] I.H. Bell, J. Wronski, S. Quoilin, V. Lemort. Pure and Pseudo-pure Fluid Thermophysical Property Evaluation and the Open-Source Thermophysical Property Library CoolProp. Industrial & Engineering Chemistry Research. 53 (2014) 2498-508.

[18] American Society of Heating Refrigerating and Air-Conditioning Engineers Inc. (ASHRAE). Designation and Safety Classification of Refrigerants. American Society of Heating, Refrigerating and Air-Conditioning Engineers, Inc. (ASHRAE), Atlanta, GA, USA, 2010.

[19] The European Parliament and the Council of the European Union. Regulation (EU) No 517/2014 on fluorinated greenhouse gases and repealing Regulation (EC) No 842/2006. Official Journal of the European Union. The European Parliament and the Council of the European Union, Strasbourg, 2014.

[20] F. Zhou, S.N. Joshi, R. Rhote-Vaney, E.M. Dede. A review and future application of Rankine Cycle to passenger vehicles for waste heat recovery. Renewable and Sustainable Energy Reviews. 75 (2017) 1008-21.

[21] CoolProp. *List of fluids*. Available at: http://www.coolprop.org/fluid_properties/PurePseudoPure.html#list-of-fluids, accessed online: 4th december 2017.

[22] S. Quoilin, S. Declaye, A. Legros, G. Ludovic, V. Lemort. Working fluid selection and operating maps for Organic Rankine Cycle expansion machines. University of Liège, Thermodynamics Laboratory, Liège, Belgium, 2012.

[23] H. Heiberg, S. Kristiansen, J. Mamen, R. Gangstø Skaland, H. Szewczyk-Bartnicka, H.T. Tilley Tajet. Været i Norge, Klimatologisk oversikt. Året 2016. Meteorologisk institutt, Oslo, 2017.

[24] E. Nygård. Batterilading i hybride fremdriftssystemer ved hjelp av tapsenergi fra forbrenningsmotoren [master thesis]. Bergen: University of Bergen; 2017. Retrieved from http://bora.uib.no/handle/1956/16070, accessed online: 11th December 2017.

[25] Z. Gao, D.E. Smith, C. Stuart Daw, K. Dean Edwards, B.C. Kaul, N. Domingo, et al. The evaluation of developing vehicle technologies on the fuel economy of long-haul trucks. Energy Conversion and Management. 106 (2015) 766-81.

[26] R. Ciconkov. Refrigerants: There is still no vision for sustainable solutions. International Journal of Refrigeration. 86 (2018) 441-8.